Available online at www.sciencedirect.com
ScienceDirect
Trans. Nonferrous Met. Soc. China 35(2025) 2332−2340
Transactions of Nonferrous Metals Society of China
www.tnmsc.cn

Effect of spherical cast WC particle on mechanical properties of WC/NiCu composites

Yu-nan FAN[1], Yong LIU[1], Ruo-chong WANG[1], Guo-feng ZHANG[1,2]

1. State Key Laboratory of Powder Metallurgy, Central South University, Changsha 410083, China;
2. Luoyang Golden Egret Geotools Co., Ltd., Luoyang 471000, China

Received 26 July 2024; accepted 28 April 2025

Abstract: A new NiCu alloy was developed and utilized as binder phase for WC composites. The composites with spherical cast WC particle contents of 55−65 wt.% were prepared by rapid hot-pressing technique. The microstructures were characterized by scanning electron microscopy (SEM), energy-dispersive X-ray spectroscopy (EDS), and transmission electron microscopy (TEM). The results reveal that the cast WC particles are uniformly dispersed within the NiCu matrix. The interface between WC and NiCu alloy is clear with no additional phase observed. Mechanical properties testing indicates that the hardness of the composite shows minimal variation as the cast WC particle content increases. Both the transverse rupture strength (TRS) and fracture toughness show a comparable decline, while the impact toughness first increases and then decreases. The NiCu alloy matrix plays a critical role in enhancing the fracture toughness of the composite. However, at high strain rates, the impact toughness deteriorates due to strain rate hardening of the NiCu matrix and a reduced density resulting from the higher WC content.

Key words: rapid hot-pressing; WC composite materials; NiCu alloy; toughness

1 Introduction

Nickel−copper (NiCu) alloys are known for their outstanding performance characteristics, including excellent corrosion resistance, high electrical conductivity, and superior thermal conductivity [1−3]. These properties make NiCu alloys suitable for a wide range of applications, such as in aerospace [4], offshore engineering [5], and oil and gas industries [6]. However, in exposure to high temperatures and harsh environments, the relatively low hardness and wear resistance of the NiCu-based alloy need to be addressed [7,8]. Recently, a new type of NiCu alloy was developed [9], which has high wear resistance and corrosion resistance at the same time.

To further enhance the mechanical properties of NiCu alloys, particle reinforcement has been widely employed. LI et al [10] studied the effect of graphene nanoplatelets on the microstructure and wear resistance of NiCu/GNPs composite coating, and showed that the microhardness of the NiCu/GNPs composite coating increased by 130%, while the wear mass loss was reduced by 936% compared with the NiCu coating. ALIZADEH and SAFAEI [11] examined the influence of the additions of Cu and Al_2O_3 on the properties of NiCu/Al_2O_3 nano-composite coatings. It was found that the microhardness, wear resistance, and corrosion resistance of the deposited coatings were increased, and the microhardness and wear resistance of the Cu/Al_2O_3 (20 g/L) nano-composite coatings increased by about 2.4 and 3.75 times, respectively.

Tungsten carbide (WC) is a type of reinforcing

Corresponding author: Yong LIU, Tel: +86-13307318308, E-mail: yonliu@csu.edu.cn
https://doi.org/10.1016/S1003-6326(25)66818-X

particle known for its outstanding wear resistance, strength, hardness and good wettability with nickel-based alloys [12−15]. WC particle reinforcement has shown apparent improvements in the mechanical properties of nickel-based alloys, for example, enhanced hardness and wear resistance, thereby effectively extending the service life [16−19]. ZHOU and DAI [20] investigated the effect of WC particle reinforcement in nickel-based alloy coatings, demonstrating that a coating without pores and cracks can be prepared using laser induction hybrid rapid cladding. DOMITNER et al [21] explored the relationship between microstructures and the hardness in Ni alloy/WC composites fabricated by the laser directed energy deposition (L-DED) method. It was indicated that the hardness of the composites is determined by both the grain size and the crystal structure of the carbides. For composites with the same crystal structure, smaller grain size generally leads to higher hardness. LI et al [22] examined the impact of WC content on the microstructure and wear performance of WC/Ni60 composites. It was found that increasing the WC content promoted the formation of new types of W-containing carbides, resulting in significant improvements in hardness, corrosion resistance, and abrasion resistance. To date, WC-reinforced nickel matrix composites have primarily been used in fused cladding layers, with only a limited number of literature reports on the bulk form. Furthermore, there is a scarcity of research on cast WC particle-reinforced NiCu alloys.

In this study, WC/NiCu composites were fabricated using rapid hot-pressing technology, and the comprehensive properties of bulk composites with varying WC contents were investigated, with NiCuSiMnB alloy serving as the metallic binder phase. The primary objective was to precisely determine the impact of WC mass fraction on the performance of the composite. To achieve high density and superior overall properties, detailed characterization and analysis of the microstructure, mechanical properties, and the interactions between the metallic binder and WC particles were conducted. Based on the experimental results and discussion, the findings provide a solid theoretical foundation for the potential application of WC/NiCu composites in bulk form for engineering components.

2 Experimental

The raw materials were NiCu alloy powder (NiCuSiMnB) with a particle size range of 53−150 μm, and spherical cast WC powder with a particle size range of 45−150 μm. Spherical cast WC powder was provided by Luoyang Golden Egret Geotools Company (China). The preparation process of NiCu alloy powder involved the following steps: firstly, the NiCu alloy was overheated to obtain molten metal, and then the molten melt was fragmented into small droplets by high-speed argon gas (Ar), and finally the droplets solidified into spherical powder particles. The morphologies of the raw materials are shown in Fig. 1. The cast WC particles exhibited a smooth surface and high sphericity. The surface of NiCu alloy particles displayed a planetary structure, which was attributed to different solidification rates of the individual particles. The chemical compositions of the two materials are given in Table 1. The raw particles were thoroughly mixed using a V-type mixing machine at a rotating speed

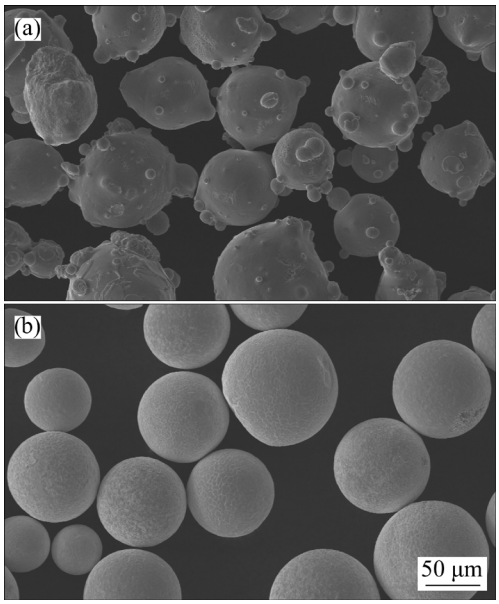

Fig. 1 SEM images of raw materials: (a) NiCu powder; (b) WC powder

Table 1 Chemical compositions of NiCu and WC raw powder (wt.%)

Powder	C	Si	B	W	Ni	Cu	Fe	Cr	Mn
NiCu	−	4	1.7	−	Bal.	28	−	−	1
WC	4.2	−	−	Bal.	−	−	0.5	0.2	−

of 50 r/min for 10 h. The WC contents were 55, 60, and 65 wt.% respectively.

The WC/NiCu composites were prepared using a rapid hot-pressing furnace (FHP−828) with a rated power of 72 kW, input voltage of 380 V, and a pressure range of 10−100 kN. During the sintering process, the sample was first heated from room temperature to 400 °C at a rate of 100 °C/min, followed by holding at 400 °C under the applied sintering pressure. The temperature was then increased to near the sintering state at a rate of 100 °C/min, and subsequently, the heating rate was reduced until the target sintering temperature was reached. The compositions and the sintering process parameters for the WC/NiCu composites are provided in Table 2.

The samples were cut, ground and polished. The relative densities of the WC/NiCu composites were determined using the Archimedes method with an electronic balance (MSA324S−000−DU). Microstructural analysis was conducted using an optical microscope (OM) and a scanning electron microscope (MIRA3 LMN SEM). The phase composition was determined using Bruker D8 ADVANCE X-ray diffraction (XRD) over an angular range from 10° to 90°. Furthermore, high-angle annular dark field scanning transmission electron microscopy (HAADF-STEM) and energy-dispersive X-ray spectroscopy (EDS) analyses were performed using a transmission electron microscope (TEM, Thermo Fisher Talos F200E) to investigate the nanoscale interfacial microstructures of WC/NiCu composites. TEM samples were prepared using a focused ion beam (FIB, Scios 2 DualBeam). Rockwell hardness testing was performed using a Hardness Tester (671HRS−150). Impact toughness was measured using an impact testing machine (XJ−40A). The transverse rupture strength (TRS) measurement was conducted using a three-point bending instrument based on Instron 3369, and the fracture toughness was measured using a three-point bending instrument based on Instron 5969.

3 Results

3.1 Microstructures and phase compositions

Figure 2 illustrates the microstructures of the composites prepared under different conditions. The final microstructures of the samples exhibit similar features under all preparation conditions, and the spherical cast WC particles and the NiCu alloy matrix can be clearly distinguished. Moreover, no distinct phase formation is observed. As shown in Fig. 2(a), at a sintering temperature of 850 °C, some regions of the composite exhibit irregularly shaped pores, primarily located at the interface between the cast WC particles and the NiCu matrix, suggesting a weak interface structure. As the sintering temperature increases, the interface between the cast WC particles and the NiCu matrix improves significantly. In Fig. 2(c), at 900 °C, the 60WC/NiCu composite exhibits improved uniformity, with no apparent pores or defects. Only a small number of spherical pores, smaller than 4 μm, are distributed in the NiCu alloy matrix. This implies that at 900 °C, the NiCu matrix offers enhanced coverage, filling the gaps between the cast WC particles and reducing pore formation. However, with increasing cast WC content, particle aggregation becomes more pronounced, leading to pore formation and aggregation at the interface, as shown in Fig. 2(d).

Figure 3 presents the HAADF-STEM image of the interface in the 60WC/NiCu composite sintered at 900 °C, along with the corresponding element distribution maps and selected area electron diffraction (SAED) pattern. The image clearly reveals a well-defined interface between the cast WC particles and the NiCu matrix, with no additional phases formed. The EDS analysis further shows that the diffusions of Ni and Cu into the

Table 2 Composition, sintering process parameters and density of WC/NiCu composites

Composite	Chemical composition/wt.%		Sintering temperature/°C	Sintering time/min	Density/ ($g \cdot cm^{-3}$)	Relative density/%
	WC	NiCu				
60WC/NiCu	60	40	850	10	11.61	98.86
55WC/NiCu	55	45	900	10	11.17	98.59
60WC/NiCu	60	40	900	10	11.72	99.80
65WC/NiCu	65	35	900	10	11.85	97.22

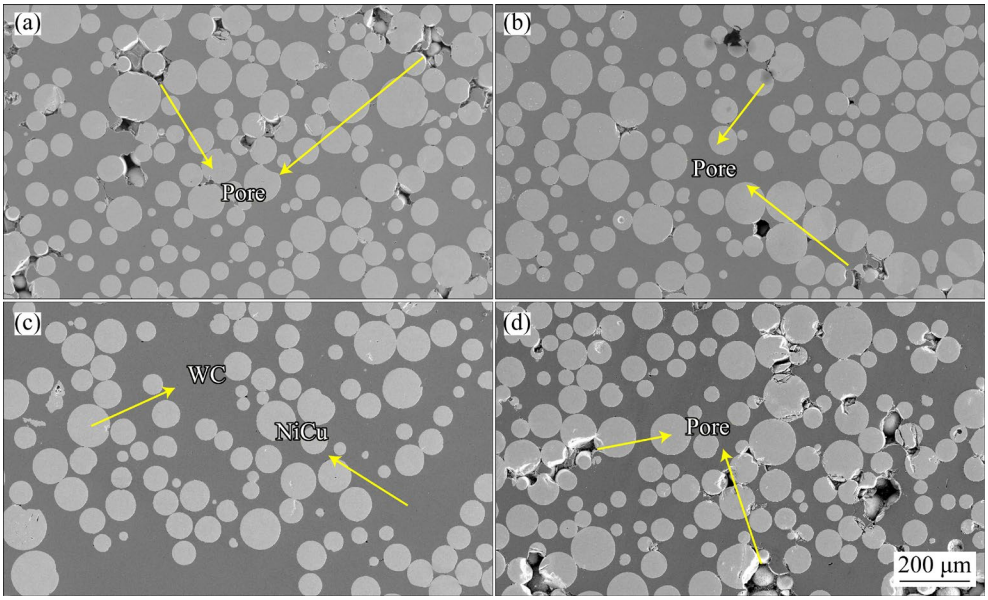

Fig. 2 Microstructures of WC/NiCu composites: (a) 60WC/NiCu (850 °C); (b) 55WC/NiCu (900 °C); (c) 60WC/NiCu (900 °C); (d) 65WC/NiCu (900 °C)

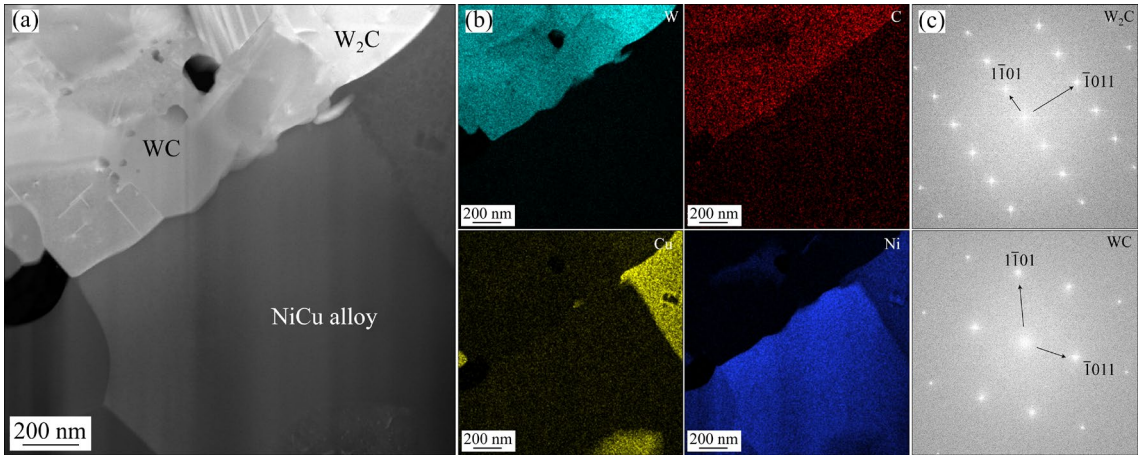

Fig. 3 HAADF-STEM image (a), corresponding element distribution maps (b) and selected area electron diffraction pattern (c) at interface in 60WC/NiCu (900 °C) composite

interface region are limited, thereby maintaining the integrity of the cast WC particles.

The XRD patterns of various composites are presented in Fig. 4. The results indicate that the main phases present in the WC/NiCu composite are WC, W_2C, NiCu, Ni_3Si, and Ni_5Si_2. As the cast WC content in the composite increases, the intensity of the WC peaks correspondingly rises, indicating that WC is well-preserved without significant decomposition or phase transformation. What's more, the sintering temperature influences the phase composition. At 900 °C, the peak intensities of the W_2C and silicide phases (Ni_3Si and Ni_5Si_2) become more prominent, suggesting that high temperatures promote partial decomposition of WC, and enhance element diffusion within the matrix phase, facilitating the formation of secondary phases.

3.2 Mechanical properties

Figure 5 illustrates the Rockwell hardness and transverse rupture strength (TRS) of the WC/NiCu composites. The results show that both hardness and transverse rupture strength increase with rising sintering temperatures. The hardness of the composites sintered at 900 °C dose not show much difference, and the composites has a hardness of HRA 78.4 at the WC content of 65 wt.%. In addition, the TRS of the composites tends to decrease

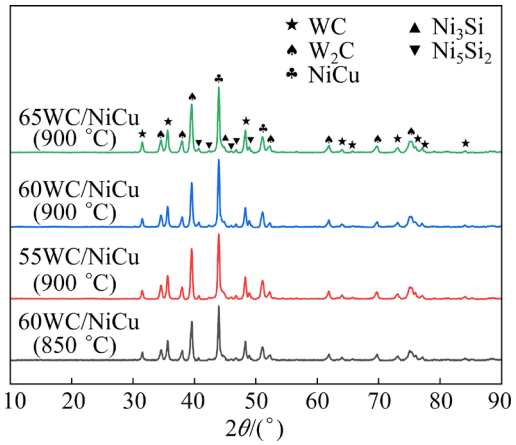

Fig. 4 XRD patterns of WC/NiCu composites

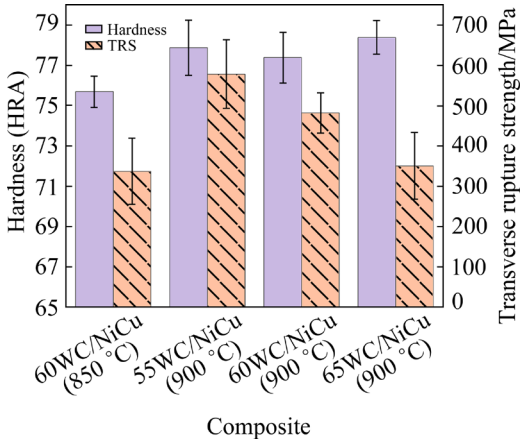

Fig. 5 Hardness and transverse rupture strength of WC/NiCu composites

as the WC content increases. This can be attributed to the distinct properties of the two phases present in WC/NiCu composites. Cast WC is the hard phase in the composite, exhibiting a higher elastic modulus than NiCu alloy. Consequently, the interface between the two phases represents a potential weak point in the composite. The deformation of cast WC particles and NiCu alloy is not coordinated, resulting in stress concentration at the interface. Although the spherical cast WC particles can effectively reduce stress concentration due to the smooth surface, an increased WC content results in a greater number of weak interfaces.

The impact toughness and fracture toughness of the composites are shown in Fig. 6. It can be seen that the impact toughness of the composites with WC contents of 60 and 65 wt.% is improved compared to that of the composite with WC content of 55 wt.%. The highest impact toughness of the 60WC/NiCu composite (sintered at 900 °C) is 0.62 J/cm^2. However, the fracture toughness of the composites decreases as the WC content increases.

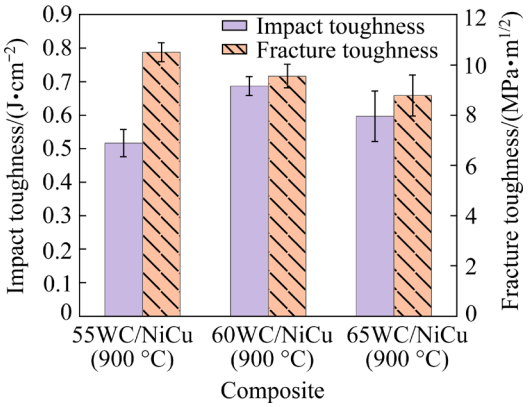

Fig. 6 Impact toughness and fracture toughness of WC/NiCu composites

Figure 7 presents the fracture morphology of WC/NiCu composites with varying cast WC contents. As shown in Fig. 7(a), the 55WC/NiCu composite exhibits pronounced porosity, cracking, and poor interface with cast WC particles. Under impact loading, the residual pores likely serve as the primary sites for micro-crack initiation, thereby reducing the overall impact toughness of the composite. With an increase in cast WC content, the 65WC/NiCu composite displays a further weakened interface compared to the 55WC/NiCu composite, with more pronounced porosity, as shown in Fig. 7(c). This incomplete interface induces cracks primarily along the boundary between the cast WC particles and the NiCu matrix. In contrast, at a WC content of 60 wt.%, Fig. 7(b) shows improved interface between the WC particles and the NiCu matrix, with no significant pores. In Fig. 7(d), cracks are observed primarily propagating through both the cast WC particles and the matrix. Additionally, the cracks exhibit deflection and branching when encountering cast WC particles.

Figure 8 illustrates the crack propagation behavior in the WC/NiCu composites. As shown, cracks initiate at specific locations near the cast WC particles, typically resulting from stress concentration. The crack propagation paths indicate that cracks predominantly propagate within the cast WC particles and the matrix, with significant branching occurring inside the WC particles, rather than along the interface between the WC particles and the NiCu matrix. This finding suggests that the cast WC particles, as the hard phase, hinder direct

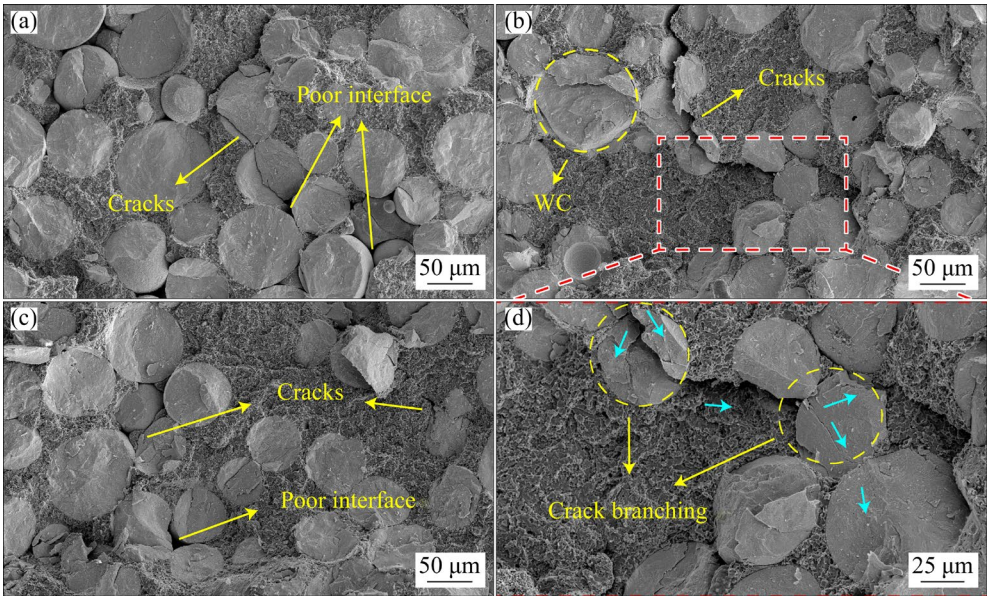

Fig. 7 Fracture morphologies of WC/NiCu composites under impact toughness: (a) 55WC/NiCu (900 °C); (b) 60WC/NiCu (900 °C); (c) 65WC/NiCu (900 °C); (d) Magnified view of (b)

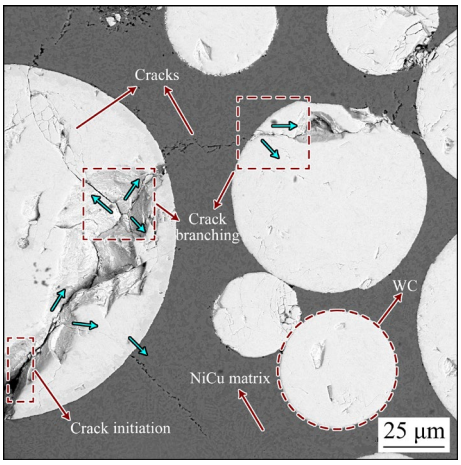

Fig. 8 Crack growth path of composite

crack propagation. Additionally, cracks in the NiCu matrix gradually become narrow as the propagation path advances.

4 Discussion

In the rapid hot-pressing sintering process, both the sintering temperature and the content of cast WC in the composite directly affect the densification of WC/NiCu composites. At lower temperatures, the interpenetration and bonding among powder particles are restricted, making it difficult to eliminate the space among particles, which leads to the formation of more pores at the interface between WC particles and the NiCu matrix. Cast WC, as a high-hardness ceramic phase, exhibits significantly lower fluidity and plasticity than the NiCu alloy matrix at high temperatures [23,24]. During the sintering process, an increased WC content restricts the flow and rearrangement of the binder phase, thereby hindering sufficient contact and densification among powder particles, and leaving more residual pores in the composite. Furthermore, a high WC content can lead to the aggregation of WC particles, increasing the number of interfaces between WC particles and the NiCu matrix. Due to the significant difference in the thermal expansion coefficients between WC particles and the NiCu matrix, high WC content exacerbates stress concentration at the interface during cooling, further deteriorating the density of the composite. Therefore, a controlled reduction in WC content can enhance the densification of the composite.

No significant diffusion of elements is observed at the interface of WC/NiCu composites. The primary factor is the insufficient diffusion temperature of W and C in the NiCu alloy. The high melting point of cast WC contributes to its chemical stability at the sintering temperature of 900 °C, making it difficult to react significantly with the NiCu matrix. Furthermore, the solubility of W in Ni and Cu is extremely limited, meaning that even with some diffusion of elements, W does not

dissolve extensively in the matrix in the form of a solid solution. Additionally, although 900 °C is high enough to facilitate the flow and formation of the NiCu alloy matrix, the relatively short sintering time in the rapid hot-pressing process is insufficient for extensive diffusion of alloy elements.

WC particles enhance the hardness of the NiCu alloy matrix by hindering dislocation motion and enhancing the resistance to deformation. Generally, the hardness of the composite increases with increasing WC content. However, as shown in Fig. 5, while the hardness of the composite tends to increase with rising WC content, the overall difference is relatively small. This can be attributed to the fact that as the WC content increases, the number of interfaces between WC particles and the NiCu matrix also increases, and the density decreases. Although the hardness increases with the rise in WC particle content, the increase in defects within the composite leads to a reduction in hardness.

The toughness of the composite is influenced by several factors, including composition, microstructure and loading conditions. In WC/NiCu composites, the NiCu matrix, with its inherent toughness, exhibits high crack resistance during crack propagation [25−28]. As a result, the NiCu matrix plays a critical role in enhancing the toughness of the composite. As cracks propagate through the NiCu matrix, the stress field at the crack tip is influenced by plastic deformation of the material, which reduces the stress concentration at the crack tip. Additionally, due to the difference in thermal expansion coefficients between WC particles and the NiCu matrix, the interfaces within the composite are generally considered weak points. As the WC content increases, the proportion of the interface in the composite also rises, along with an increase in porosity. Under quasi-static loading, the crack propagation rate is slow, and the stress concentration at the pores gradually accumulates, promoting the crack to propagate along irregular paths through the pores. The combined effects of these factors ultimately result in a decrease in fracture toughness as the WC content increases.

However, the impact toughness of the composite increases initially and then decreases as the WC content rises. This behavior can be attributed to the significant difference in the deformation behavior of materials under high strain rates compared to quasi-static loading. Under impact loading, NiCu alloys exhibit strain rate hardening, meaning that the strength of the material increases with the loading rate, but plasticity decreases. Consequently, when the content of the NiCu matrix is relatively high, the impact toughness decreases. Additionally, at high strain rates, the short duration of load application prevents sufficient plastic deformation of the NiCu matrix. Therefore, a moderate increase in WC content can improve impact toughness. However, excessively high WC content can lead to increased porosity, resulting in local stress concentration and creating sites for micro-crack initiation, thereby reducing impact toughness.

FERNÁNDEZ et al [29] found that the hardness values of the WC/Ni60 coating material are HV 515−563. By comparison, the hardness of present WC/NiCu composites are very close (HV 560−595). However, considering the fact that WC/NiCrBSi composites are widely used as coating materials with poor toughness, the WC/NiCu composites in bulk form may have much more applications for engineering components.

5 Conclusions

(1) The 60WC/NiCu composite exhibits a uniform microstructure and high density, with only a few spherical pores in the NiCu alloy matrix. The cast WC particles maintain the spherical shape, with no distinct phases formed at the interface.

(2) Due to the low solubility of W in Ni and the high melting point of WC, which provides high chemical stability during sintering, no significant element diffusion occurs at the interface between WC particles and the NiCu matrix.

(3) The composites have a high hardness of HRA 78.3 at a WC content of 65 wt.%. With increasing WC content, the transverse rupture strength and fracture toughness of the composite decrease, while the impact toughness first increases and then declines.

(4) The NiCu matrix plays a crucial role in improving the fracture toughness of the composite.

(5) At high strain rates, the impact toughness of the composite is primarily governed by two factors: the strain rate hardening of the NiCu matrix and the decreased densification caused by the high WC content.

CRediT authorship contribution statement

Yu-nan FAN: Methodology, Investigation, Data curation, Visualization, Formal analysis, Writing – Original draft, Writing – Review & editing; **Yong LIU:** Writing – Review & editing, Funding acquisition, Project administration, Resources, Supervision; **Ruo-chong WANG:** Methodology, Resources; **Guo-feng ZHANG:** Methodology, Resources.

Declaration of competing interest

The authors declare that they have no known competing financial interests or personal relationships that could have appeared to influence the work reported in this paper.

Acknowledgments

This research was supported by the National Key Research and Development Program of China (No. 2021YFB3701801), and the Regional Innovation and Development Joint Fund of National Natural Science of China (No. U20A20236).

References

[1] SUNDARAM M, KAMARAJ A B, LILLIE G. Experimental study of localized electrochemical deposition of Ni−Cu alloy using a moving anode [J]. Procedia CIRP, 2018, 68: 227−231.

[2] LI Bao-song, MEI Tian-yong, LI Dan-dan, DU Sheng-song, ZHANG Wei-wei. Structural and corrosion behavior of Ni−Cu and Ni−Cu/ZrO_2 composite coating electrodeposited from sulphate-citrate bath at low Cu concentration with additives [J]. Journal of Alloys and Compounds, 2019, 804: 192−201.

[3] HEDAYATI K. Structural and magnetic characterization of electrodeposited Ni−Cu/Cu and Fe−Ni−Cu/Cu multilayer [J]. Applied Physics A, 2014, 118: 975−979.

[4] ZHU Yu-liang, ZHENG Wen-jie, SONG Zhi-gang, FENG Han. Development and application of nickel-copper alloy in China [J]. Hot Working Technology, 2019, 48: 23−26. (in Chinese)

[5] ORIŇÁKOVÁ R, TUROŇOVÁ A, KLADEKOVÁ D, GÁLOVÁ M, SMITH R M. Recent developments in the electrodeposition of nickel and some nickel-based alloys [J]. Journal of Applied Electrochemistry, 2006, 36: 957−972.

[6] GHOSHA S K, GROVER A K, DEY G K, TOTLANI M K. Nanocrystalline Ni−Cu alloy plating by pulse electrolysis [J]. Surface Coatings Technology, 2000, 126: 48−63.

[7] ZHUANG Qi-ren, HUANG Li-min, ZHANG Wen-zhen. Effect of rare earth and ceramic on the microstructure and properties of laser cladding Monel alloy coatings [J]. Journal of Optoelectronics Laser, 2000, 11: 309−312. (in Chinese)

[8] LAI Peng-fei, ZHONG Min, WU Yuan, CHEN Wei, LI Li-hong, LUO Zong-qiang, ZHANG Wei-wen. Study on interface characteristics of casting copper water jacket with pre-embedded monel tube [J]. Hot Working Technology, 2019, 48: 30−34. (in Chinese)

[9] LIU Yong, WANG Ruo-chong. A wear and corrosion resistant Ni−Cu alloy and its preparation method, CN116334449A [P]. 2023−04−04.

[10] LI Hui-dong, XIA Ye-lin, XIE Min, SHI Chuan, LEI Jian-bo. Graphene nanoplatelets reinforced NiCu composite manufactured by laser melting deposition [J]. Journal of Alloys and Compounds, 2022, 929: 167261.

[11] ALIZADEH M, SAFAEI H. Characterization of Ni−Cu matrix, Al_2O_3 reinforced nano-composite coatings prepared by electrodeposition [J]. Applied Surface Science, 2018, 456: 195−203.

[12] ZHANG Teng, ZHOU Jian-zhong, WANG Ji-zhuang, MENG Xian-kai, LI Peng-fei, HUANG Shu, ZHU Hao. Effect of hybrid ultrasonic-electromagnetic field on cracks and microstructure of Inconel 718/60%WC composites coating fabricated by laser cladding [J]. Ceramics International, 2022, 48: 33901−33913.

[13] CHEN Hong-yu, GU Dong-dong, KOSIBA K, LU Ti-wen, DENG Liang, XI Li-xia, KÜHN U. Achieving high strength and high ductility in WC-reinforced iron-based composites by laser additive manufacturing [J]. Additive Manufacturing, 2020, 35: 101195.

[14] RASHID H, LUO Xiao-tao, DONG Xin-yuan, ZHANG Li, LI Chang-jiu. Plasma-sprayed Al-based coating with WC-addition for excellent corrosion resistance and enhanced wear protection of Mg alloys [J]. Transactions of Nonferrous Metals Society of China, 2024, 34: 2275−2288.

[15] MIN Fan-lu, YU Song-bai, WANG Sheng, YAO Zhan-hu, NOUDEM J G, LIU Si-jin, ZHANG Jian-feng. Preparation and properties of Ni-coated WC powder and highly impact resistant and corrosion resistant WC−Ni cemented carbides [J]. Transactions of Nonferrous Metals Society of China, 2022, 32: 1935−1947.

[16] XU Pei-hua, ZHU Li-da, XUE Peng-sheng, YANG Zhi-chao, WANG Shu-hao, NING Jin-sheng, MRNG Gui-ru, LAN Qing, QIN Shao-qing. Microstructure and properties of IN718/WC-12Co composite coating by laser cladding [J]. Ceramics International, 2022, 48: 9218−9228.

[17] WANG Qian, LI Qian, ZHANG Liang, CHEN Dong-xu, JIN Hui, LI Ji-dong, ZHAGN Jun-wei, BAN Chun-yan. Microstructure and properties of Ni−WC gradient composite coating prepared by laser cladding [J]. Ceramics International, 2022, 48: 7905−7917.

[18] CHEN Hong-yu, GU Dong-dong, ZHANG Hong-mei, XI Li-xia, LU Ti-wen, DENG Liang, KÜHN U, KOSIBA K. Novel WC-reinforced iron-based composites with excellent mechanical properties synthesized by laser additive manufacturing: Underlying role of reinforcement weight fraction [J]. Journal Materials Processing Technology, 2021, 289: 116959.

[19] CHEN Hong-yu, GU Dong-dong, DENG Liang, LU Ti-wen, KÜHN U, KOSIBA K. Laser additive manufactured high-performance Fe-based composites with unique strengthening structure [J]. Journal of Materials Science & Technology, 2021, 89: 242−252.

[20] ZHOU Sheng-feng, DAI Xiao-qin. Laser induction hybrid rapid cladding of WC particles reinforced NiCrBSi

composite coatings [J]. Applied Surface Science, 2010, 256: 4708−4714.

[21] DOMITNER J, SILVAYEH Z, BUZOLIN R H, KRISAM S, ACHTERHOLD K, POVODEN-KARADENIZ E, SOMMITSCH C, MAYR P. Microstructure characterization of nickel matrix composite reinforced with tungsten carbide particles and produced by laser cladding [J]. Advanced Engineering Materials, 2022, 24: 2200463.

[22] LI Wan-yang, YANG Xue-feng, XIAO Ju-peng, HOU Qi-min. Effect of WC mass fraction on the microstructure and friction properties of WC/Ni60 laser cladding layer of brake discs [J]. Ceramics International, 2021, 47: 28754−28763.

[23] ZHANG Zhi-guo, ZHANG Bei, LI Wei. Wear behaviors of WC particle reinforced Cu composites under electrical current [J]. Transactions of Materials and Heat Treatment, 2016, 37(5): 17−21. (in Chinese)

[24] HU Yong, WANG Liang, LOU Fu-xing, XIA Hong-chao, ZHANG Qun-li, YAO Jian-hua. Mechanism study of steady magnetic field effect on spherical WC particle distribution during laser melt injection [J]. Journal of Mechanical Engineering, 2021, 57: 240−248.

[25] LI An-hai, ZHAO Jun, WANG Dong, GAO Xin-liang, TANG Hong-wei. Three-point bending fatigue behavior of WC−Co cemented carbides [J]. Materials & Design, 2013, 45: 271−278.

[26] LUO Wen-yan, LIU Yun-zhong, SHEN Jun-jian. Effects of binders on the microstructures and mechanical properties of ultrafine WC-10%Al_xCoCrCuFeNi composites by spark plasma sintering [J]. Journal of Alloys and Compounds, 2019, 791: 540−549.

[27] MIKADO H, ISHIHARA S, OGUMA N, MASUDA K, KITAGAWA S, KAWAMURA S. Effect of stress ratio on fatigue lifetime and crack growth behavior of WC−Co cemented carbide [J]. Transactions of Nonferrous Metals Society of China, 2014, 24: 14−19.

[28] TARRAGO J M, COUREAUX D, TORRES Y, JIMÉNEZ-PIQUÉ E, SCHNEIDER L, FAIR J, LLANES L. Strength and reliability of WC-Co cemented carbides: Understanding microstructural effects on the basis of R-curve behavior and fractography [J]. International Journal of Refractory Metals and Hard Materials, 2018, 71: 221−226.

[29] FERNÁNDEZ M R, GARCÍA A, CUETOS J M, GONZÁLEZ R, NORIEGA A, CADENAS M. Effect of actual WC content on the reciprocating wear of a laser cladding NiCrBSi alloy reinforced with WC [J]. Wear, 2015, 324: 80−89.

球形铸造 WC 颗粒对 WC/NiCu 复合材料力学性能的影响

范语楠[1]，刘　咏[1]，王若冲[1]，张国锋[1,2]

1. 中南大学 粉末冶金国家重点实验室，长沙 410083；
2. 洛阳金鹭硬质合金工具有限公司，洛阳 471000

摘　要：开发了一种新型 NiCu 合金，并将其作为 WC 复合材料的粘结相。通过快速热压技术制备了铸造 WC 含量为 55%~65%(质量分数)的复合材料。采用扫描电子显微镜(SEM)、能量色散 X 射线光谱仪(EDS)和透射电子显微镜(TEM)对复合材料的微观结构进行了表征。结果表明，铸造 WC 颗粒在 NiCu 基体中分布均匀，且 WC 与 NiCu 合金之间的界面清晰，未形成附加相。力学性能测试结果显示，随着铸造 WC 颗粒含量的增加，复合材料的硬度变化幅度较小，横向断裂强度(TRS)和断裂韧性呈现出相似的下降趋势，而冲击韧性则呈现出先增加后下降的趋势。NiCu 合金基体在提升复合材料断裂韧性方面起到了关键作用；而在高应变速率下，NiCu 基体的应变速率硬化效应以及高 WC 含量引起的密度降低共同导致了冲击韧性的下降。

关键词：快速热压；WC 复合材料；NiCu 合金；韧性

(Edited by Bing YANG)